ICIC Express Letters
Part B: Applications
Volume **11**, Number **10**, October **2020**

ICIC International ©2020 ISSN 2185-2766
pp. **929–937**

A NOVEL GAIT-SPEED RECOGNITION APPROACH BASED ON IMPROVED PARTICLE FILTER FOR OMNIDIRECTIONAL SUPPORT WALKER

Yatian Gao[1], Junyou Yang[1], Yina Wang[1], Donghui Zhao[1]
and Shuoyu Wang[2]

[1]School of Electrical Engineering
Shenyang University of Technology
No. 111, Shenliao East Road, Shenyang 110870, P. R. China
higaoyatian@163.com; junyouyang@sut.edu.cn; wangyina0402@gmail.com

[2]School of Systems Engineering
Kochi University of Technology
185 Miyanokuchi, Tosayamada-cho, Kami-shi, Kochi 782-8502, Japan
Wang.shuoyu@kochi-tech.ac.jp

Received March 2020; accepted June 2020

Abstract. *It is crucial for the omnidirectional support walker (OSW) to achieve safe and compliant control strategy based on user's walking intention. However, there is still a big challenge for compliant control because of the accurate recognition of gait speed and the poor user experience from the complex wearing of sensors. In this paper, we developed a laser sensor and proposed an improved particle filter to identify user's walking speed intention with a non-contact approach. The concept of secondary particle is introduced to improve the resampling method of particle filter aimed at overcoming the loss of particle's diversity and improving the accuracy of following. Finally, we implemented the comprehensive experiment and comparison test. Results proved the superiority of our proposed approach.*
Keywords: Omnidirectional walker, Speed intention identification, Particle filter, Secondary particle

1. **Introduction.** With an aging society and rising labor costs, especially the shortage of professional nurses [1], it has become a strong desire in the field of robotics to replace human assistance with intelligent auxiliary equipment to assist the elderly or disabled in daily life, which has a huge market prospect and research value. Various intelligent walkers with compliance and excellent recognition effect of motion intention have been developed to assist users completing auxiliary walking with poor walking capability [2]. In previous studies, friendly interface and recognition accuracy have been widely considered in intelligent walkers. In Tat et al.'s research [3], a new system was developed using the measurement of subject's resultant arm upper extremity loads. Jiang and Wang [4] designed the forearm pressure detection system based on fuzzy inference to sense the direction of the users' motion. In the experiment process, significant changes of resultant forces were observed. The recognition effect is significant, but too much attention is concentrated on the upper limb during walking, and thereby the training effect on the lower limb is weakened. In [5,6], the wearable auxiliary walker and direct detection of surface electromyography (sEMG) are applied to the walking assist process. The intention recognition effect based on support vector machine or BP neural network is significant. However, complex dressing is unfriendly. Valadao [7] designed a new controller, laser range finder and ultrasound are used to detect user's leg, whose distances from the laser sensor

DOI: 10.24507/icicelb.11.10.929

provide the information necessary to the controller. There is neither a sensor attached to the user's body nor force sensors attached to the arm supports of the walker.

In recent studies, non-contact sensors have been widely used in active controlled human interaction system, Xu et al. [8] and Weon and Lee [9] used low-cost light detection, ranging sensor, inertia measurement units and Kinect to detect the lower limb of users respectively. It retains the normal walking habits of users better. However, a large amount of computation and interference bring great challenges to its accuracy and security. In addition, the comfort and compliance of the user during walking are not considered very well. The compliant control is proposed to improve the interaction and the accuracy of intention recognition. In particular, the OSW can follow user's walking intention without additional thrust or manipulation. Therefore, it is extremely convenient and reliable that an accurate and non-contact interface is designed to recognize the walking speed intention [10].

In this paper, a single laser sensor is mounted at the bottom of the OSW to obtain the users' lower limb movement characteristics. It will be described in detail in Section 2. In Section 3, an improved particle filter is proposed to estimate and predict the motion intention dynamically. And the proportion integration differentiation feedback motion control function is applied to adjusting the motion of the walker according to the user's behavior. Then, we performed comprehensive and comparison experiments to demonstrate their effectiveness in our laboratory environment. At last, we conclude the paper in Section 5.

2. **The Omnidirctional Support Walker.** The OSW has four omni-wheels with driving motors which can move omni-directionally in narrow space without turning radius as shown in Figure 1. It is widely used in various intelligent medical places, such as intelligent nursing homes, and intelligent hospitals.

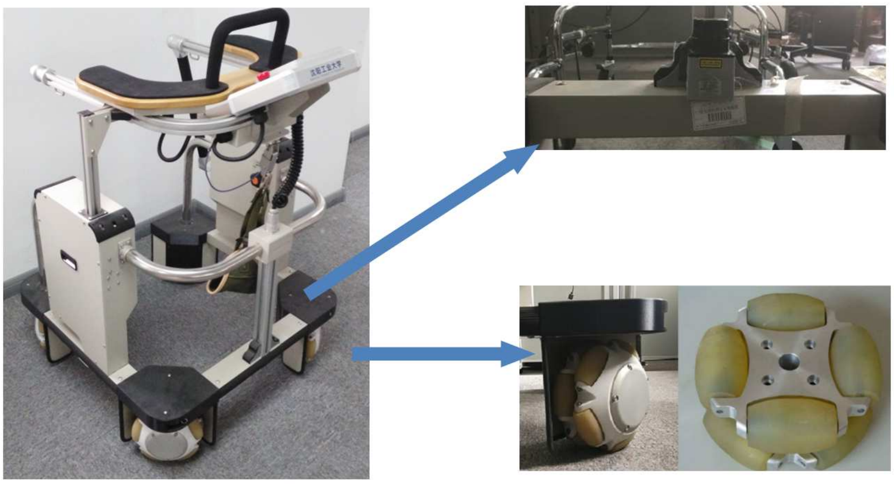

Figure 1. The structure of OSW and omni-directional wheel

The height of OSW can be adjusted to adapt to different user heights (900-1200mm). The limit of OSW speed is 0.25m/s to ensure the safety of users. The laser sensor is installed in the position shown in Figure 2. The sampling time of laser sensor is 100ms, measuring range is 240°, 4000mm. A single laser senor can cover the user's normal walking range. In this paper, the lower limb is regarded as a cylinder. We use the clustering principle and the perimeter angle theorem to represent the user's lower limb feature points as the center points of the equivalent model as shown in Figure 2.

The user's active area is limited to the angle range shown in Figure 3 due to the safe mechanical structure. Therefore, we consider the $\pm 60°$ area with the axis line of the position of the laser sensor as the effective sampling range. The laser sensor collects the lower

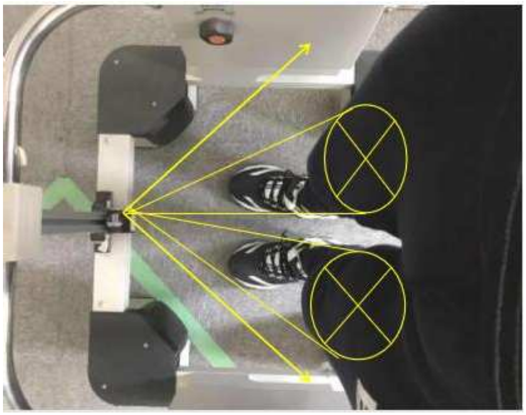

FIGURE 2. Equivalent model

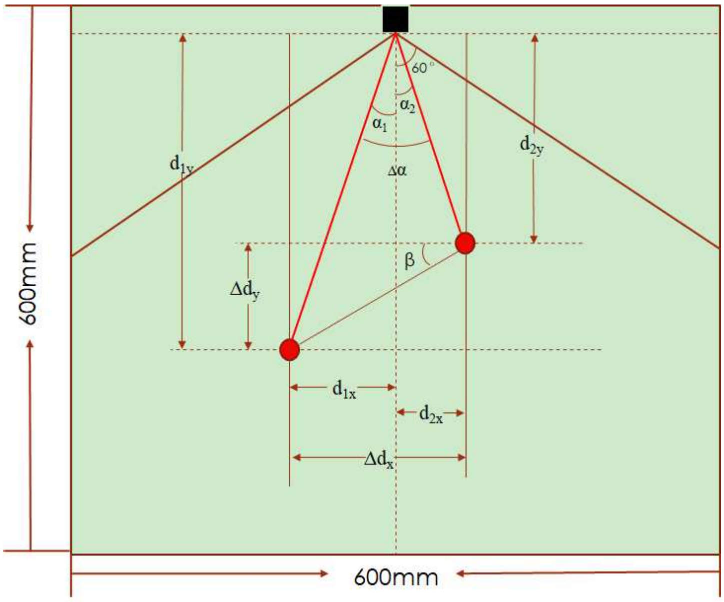

FIGURE 3. Design of interaction mode

limb movement information of the user and returns the polar coordinate data composed of angle and distance values. Specifically, we focus on the change of user's moving speed. Therefore, in order to improve analysis efficiency, coordinate transformation is necessary. Parameters can be used as motion information as shown in Figure 3.

The red points in Figure 3 represent the user's lower limbs, where α_1 and α_2 represent the angle between the lower limb and the laser sensor respectively. The angle can be computed as

$$\alpha_1 = \left(P_i^1 - 171\right) \cdot K_\alpha \tag{1}$$

$$\alpha_2 = \left(171 - P_i^2\right) \cdot K_\alpha \tag{2}$$

then, $\Delta\alpha$ can be computed, $\Delta\alpha$ represents the relative angle of two feet, and L_1, L_2 represent the distance between the lower limb and the laser sensor, which is obtained directly from the measurement. From these, we can get the vertical distance of the lower limb to the laser sensor,

$$d_{1y} = L_1 \cdot \cos\alpha_1 \tag{3}$$

$$d_{2y} = L_1 \cdot \cos\alpha_2 \tag{4}$$

then Δd_y can be computed, and the horizontal distance of the user's feet on the 2D plane also can be computed. The above parameters based on Figure 3 can be regarded as the eigenvalues of user motion information.

The control system of OSW includes laser sensor, main controller and driving motors. As shown in Figure 4, the user's walking state is captured by the laser sensor and used as the input of the main controller after coordinate transformation, filtering and feature extraction.

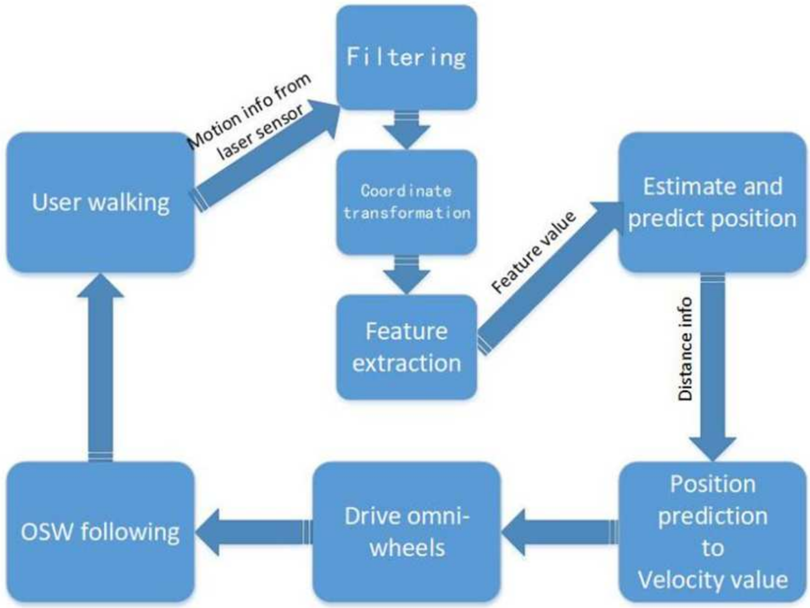

FIGURE 4. Compliance control system of OSW

Then, an improved particle filter is proposed to predict user location based on input distance value. Finally, the output position information is converted into the speed value to drive the motor of omni-wheels.

3. **Gait Speed Recognition Based on Improved Particle Filter Method.** Particle filter uses prior information and observation information [11] to predict the optimal location of pedestrians under the Bayesian framework. In this section, we explain overall framework and the concept of secondary particle into the particle filter method to solve the problem of the lack of diversity of particle filter and improve the recognition rate of the control system.

Firstly, we consider the center of the feet equivalent model as the feature point, such as p_l and p_r in Figure 5. Then, p_b can be calculated as the midpoint on the line segment based on p_l and p_r. Specifically, $p_b = (x_b, y_b)$ is regarded as the body position.

The coordinate value as the feature point at time t, is represented as a set of n samples,

$$s_t^{(i)} = \left\{ \boldsymbol{x}_t^{(i)} \quad w_t^{(i)} \right\} \quad (i = 1, 2, \ldots, n) \tag{5}$$

And each sample is treated as a particle composed of plane coordinates and weights, where i denotes the i-th particle.

$$\boldsymbol{x}_t^{(i)} = \left[x_t^{(i)} \quad y_t^{(i)} \right]^T \tag{6}$$

$\boldsymbol{x}_t$ is defined as process state vector X_t. P_b denotes the body position of the current state, and P_p is regarded as the prediction position at $t+1$ based on P_b. Besides, the sensor observation vector for measurement value $\boldsymbol{m}_t$ is defined as M_t.

To estimate the posterior probability $P(X_t|M_t)$ of X_t given M_t, we need to calculate as follows to build a desired model.

1) *Initialization.* We set the number of n initial particles to represent the body position at t_0, which are denoted by $\left\{ s_{0|0}^i | 1 \leq i \leq n \right\}$, and $\boldsymbol{x}_0^{(i)}$ is obtained through sampling

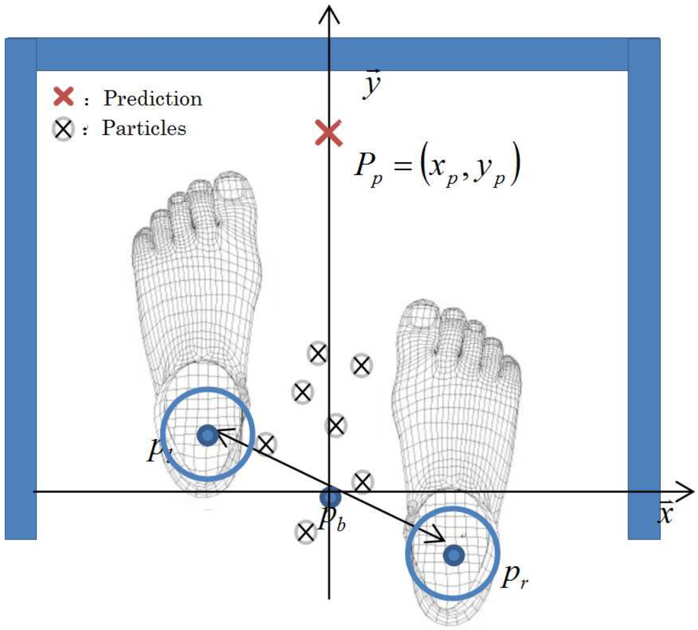

FIGURE 5. Estimation of body position

drawn from a Gaussian distribution with the variance vector σ_0^2 and the mean vector μ_0. Moreover, its weight value is constant with equal magnitude [12].

2) *Computation of the posterior probability.* The mathematical model representing the process of lower limb movement is described as follows:

$$\boldsymbol{x}_{t|t-1}^{i} = \begin{bmatrix} x_{t|t-1}^{(i)} \\ y_{t|t-1}^{(i)} \end{bmatrix} = \begin{bmatrix} x_{t-1|t-1}^{(i)} \\ y_{t-1|t-1}^{(i)} \end{bmatrix} + \begin{bmatrix} u_{x,t-1}^{(i)} \\ u_{y,t-1}^{(i)} \end{bmatrix} \tag{7}$$

The state at time t is considered to be only related to the state at time $t-1$ and the process random noise. Then the posterior probability can be calculated:

$$p^{(i)}(X_t|M_t) = \frac{1}{\sqrt{2\pi\sigma_s}} \exp\left(-\frac{D^{(i)^2}}{2\sigma_s^2}\right) \tag{8}$$

where σ_s denotes the standard deviation for the permissible location error. In addition, the Euclidean distance $D^{(i)}$ between $\boldsymbol{m}_t$ and $\boldsymbol{x}_t^{(i)}$ is defined as:

$$D_k^{(i)} = \left\|\boldsymbol{x}_{t|t-1}^{(i)} - \boldsymbol{m}_t\right\| \tag{9}$$

3) *Computation of the weight value.* The associated weight value is computed:

$$w_t^{(i)} = \frac{p^{(i)}(X_t|M_t)}{\sum_{i=1}^{n} p^{(i)}(X_t|M_t)} \tag{10}$$

4) *An improved resampling method based on secondary particles.* In previous studies, SIR particle filter algorithm was used to solve the problem of particle degradation, and it increased the computational efficiency and reduced the deviation. However, it will cause the loss of particle's diversity [13]; concretely, the resampling method based on importance leads to most particles have the same weight. It makes specific problems: when the legs are too close to each other or disturbance occurs, the tracking effect will be reduced. There will be a huge challenge to the security and compliance of the system. Therefore, we introduce the concept of secondary particles to improve the problem.

The concept of secondary particles refers that we generate new particles around the original particles by considering both weight values and Gaussian distribution principle randomly in the process of resampling. According to the rules of resampling weight allocation, the sum of the weights of the n particles at time t is 1. Therefore, we can divide $[0, 1]$ into n parts according to the particle weights:

$$\left\{ \left[0, w^1\right], \left[w^1, w^1 + w^2\right], \ldots, \left[\sum_{i=1}^{N-1} w^i, \sum_{i=1}^{N} w^i\right] \right\} \tag{11}$$

Then a random value u_i is generated in the interval to mark the reserved particle. In particular, if u_i is included in the interval i, then the particle s_t^i whose weight is w_i is retained and generated as secondary particle. After N times generation, if u_i fall in the interval n^i times, s_t^i will generate n^i secondary particles. And the secondary particles satisfy the normal distribution as follows:

$$\tilde{s}_t^i \sim N\left(s_t^i, \alpha^2\right) \tag{12}$$

The mean of the distributions is s_t^i, and the variance is α^2. It is determined by the degree of particle degradation and variance of state variables.

After introducing the second-order particles, the particles with large weights will generate more particles with high probability in the resampling stage. It avoids particle degradation and increases the diversity of particles by increasing the randomness of resampling.

5) *Estimation and prediction of body position.* The resampled particles are used to estimate and predict the user's body position.

$$\hat{\boldsymbol{x}}_t = \frac{1}{n} \sum_{i=1}^{n} \boldsymbol{x}_{t|t}^{(i)} \tag{13}$$

Then repeat the above steps and iterate to obtain continuous prediction information. The position prediction is

$$\tilde{\boldsymbol{x}}_{t|t} = \begin{bmatrix} \hat{x}_t \\ \hat{y}_t + \dot{y}\delta t \end{bmatrix} \tag{14}$$

δt represents the sampling period.

4. **Experiments and Results.**

In this section, we will verify the effectiveness and superiority of the improved algorithm based on PID controller in the laboratory environment. Firstly, we conducted an OSW compliance control experiment to verify the effectiveness of the improved algorithm.

As shown in Figure 6, six 20s healthy subjects were asked to move forward/backward, mimicking the gait of older adults with as little exposure to OSW as possible. During the experiment, the input of the control system is only acquired by the laser sensor.

The snapshots in Figure 7 represent four typical motion states, each point represents a particle, and the initial distribution of particles is shown in Figure 7(a).

At the beginning of the experiment, the subject was standing in the center of the OSW, and through the detection of the lower limb by the laser sensor, the improved particle filter

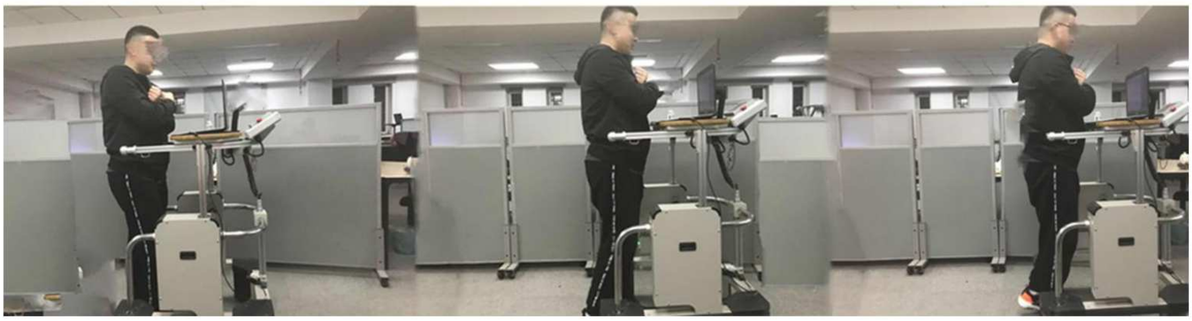

Figure 6. Forward movement experiment in lab-environment

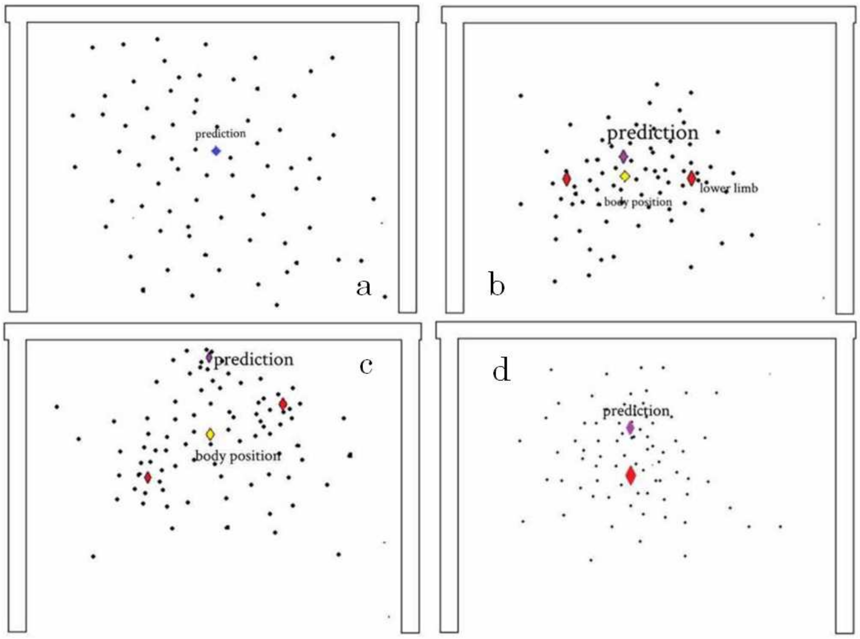

Figure 7. Motion state identification of typical state

algorithm can estimate the user's body position and thus obtain the predicted information as shown in Figure 7(b). When the subject starts to walk, its particle distribution and estimate position is shown in Figure 7(c). Specially, when the legs alternate in walking, both of legs are too close to be distinguished by the laser sensor as shown in Figure 7(d), but the improved algorithm can still get a better prediction effect. As the movement state of users changes continuously, the laser sensor captures real-time information as input constantly. Then, the prediction can be calculated by the algorithm constantly.

Then, we compared compliance differences by having subjects operate OSW in the normal way under different algorithms. To make comparison easier, data on the start and near the completion of walking were excluded. 30s of movement was performed and the results were as shown in Figure 8.

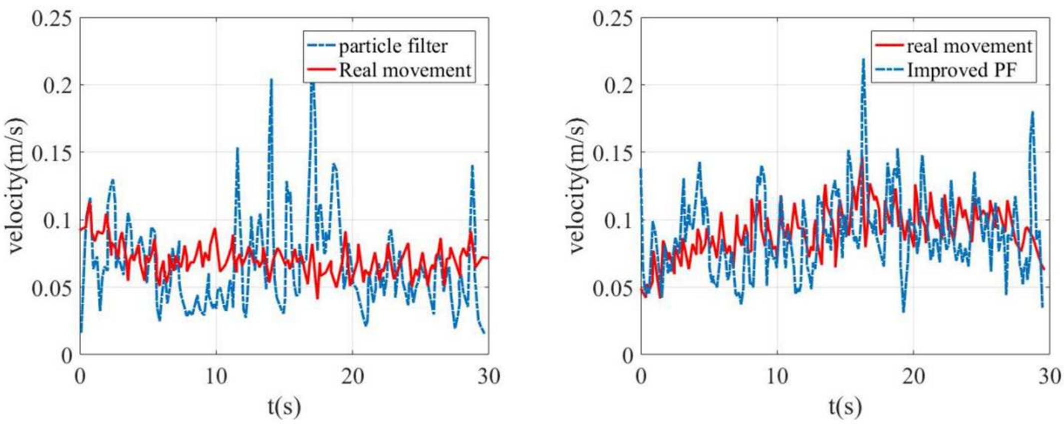

Figure 8. Experimental results based on particle filter algorithm and improved particle filter algorithm

As shown in Figure 8, the red solid line represents the actual movement of users, and the blue dashed line represents the recognition of OSW in different compliant control systems. It is obvious that the improved algorithm has excellent following effect. However, the system still overshot when the user accelerated between 15s and 20s. It may have a negative impact on user's feeling.

Then, we analyzed the subjective feelings of the subjects through questionnaires. During the experiment, subjects were not specifically informed of the experimental group (PF or IPF). This helps us to get a fair result in the process of investigation.

As shown in Figure 9, we asked subjects to rate them from the following four aspects respectively (10 points). Subjective evaluation proves that the improved particle filter algorithm optimizes the user's experience.

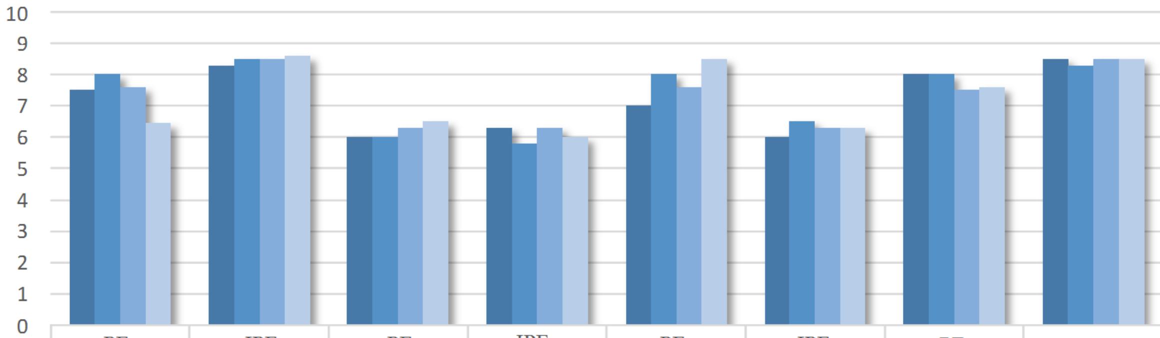

	Degree of intention recognition PF	Degree of intention recognition IPF	Pull felling PF	Pull felling IPF	Additional thrust PF	Additional thrust IPF	Degree of compliance PF	Degree of compliance IPF
A	7.5	8.3	6	6.3	7	6	8	8.5
B	8	8.5	6	5.8	8	6.5	8	8.3
C	7.6	8.5	6.3	6.3	7.6	6.3	7.5	8.5
D	6.45	8.6	6.5	6	8.5	6.3	7.6	8.5

FIGURE 9. Subjective comfort survey

Finally, the two algorithms were evaluated comprehensively by combining subjective scoring and accuracy.

According to the experience, the difference value between user speed and the OSW following speed $\Delta v \le 0.1$m/s is considered as accurate identification to user's intention. Based on the experimental results, we can obtain the correct rate of both algorithms. The results are shown in Table 1. Both algorithms have excellent operability and accuracy, especially the improved algorithm has better performance.

TABLE 1. Comprehensive evaluation of the two algorithms

Algorithm	Subjective evaluation	Correct rate
Particle filter	7.42	82.4%
Improved particle filter	8.61	88.9%

5. **Conclusion and Future Work.** The main contribution of this study is the proposal of a method for identifying users' speed intent based on improved particle filter. The results show that the method improved the accuracy and operation feeling. The interface can improve the compliance of the system. What is more, we will consider more details to improve the using quality in the future work. The transient instability of user acceleration needs to be further improved. Besides, the safety of the user's moving state in daily training still needs to be considered.

REFERENCES

[1] L. Peng and Z. G. Hou, Physical interaction methods for rehabilitation and assistive robots, *Automatica Sinica*, vol.11, no.4, pp.2000-2010, 2018.

[2] D. P. Losey, C. G. McDonald, E. Battaglia and M. K. O'Malley, A review of intent detection, arbitration, and communication aspects of shared control for physical human-robot interaction, *Applied Mechanics Reviews*, vol.70, no.1, pp.12-19, 2018.

[3] C. C. Tat, S. Parasuraman and M. K. Khan, Walking support system of ageing community, *IEEE International Conference on Recent Trends in Electrical, Control and Communication (RTECC)*, pp.28-34, 2018.

[4] Y. L. Jiang and S. Y. Wang, A novel direction control method for walking support with an ominidirectional walker, *Mecharonics and Automation*, vol.314, no.12, pp.244-252, 2014.

[5] C. Valadao, E. Caldeira, T. Bastos-Filho and A. Frizera-Neto, A new controller for a smart walker based on human-robot formation, *Sensors*, vol.16, no.7, pp.153-161, 2016.

[6] B. E. Lawson, J. Mitchell, D. Truex, A. Shultz, E. Ledoux and M. Goldfarb, A robotic leg prosthesis: Design, control, and implementation, *IEEE Robotics and Automation Magazine*, vol.21, no.4, pp.70-81, 2016.

[7] F. Negro, S. Muceli and M. Castronovo, Multi-channel intramuscular and surface EMG decomposition by convolutive blind source separation, *Journal of Neural Engineering*, vol.13, no.2, 2016.

[8] W. X. Xu, J. Huang and L. Cheng, A novel coordinated motion fusion-based walking-aid robot system, *Sensors*, vol.18, no.9, pp.256-273, 2018.

[9] L. S. Weon and S. G. Lee, Intelligent robotic walker with actively controlled human interaction, *Etri Journal*, vol.40, no.4, pp.522-530, 2018.

[10] W. X. Xu and J. Huang, Reinforcement learning-based shared control for walking-aid robot and its experimental verification, *Advanced Robotics*, vol.29, no.22, pp.1463-1481, 2015.

[11] S. J. Lee and M. Won, A vision based people tracking and following for mobile robots using CAMSHIFT and KLT feature tracker, *Journal of Korea Multimedia Society*, vol.17, no.7, pp.174-188, 2015.

[12] E. Aguirre, S. M. Garcia and J. Plata, Leg detection and tracking for a mobile robot and based on a laser device, supervised learning and particle filtering, *Proceedings of the 2nd Iberian Robotics Conference – Adcances in Robotics*, Lisbon, Portugal, pp.645-657, 2016.

[13] X. Wang and Z. M. Tang, Modified particle filter-based infrared pedestrian tracking, *Infrared Physics and Technology*, vol.53, no.4, pp.280-287, 2010.

[14] J. Yim and S. Jeong, Improvement of Kalman filters for WLAN based indoor tracking, *Expert Systems with Applications*, vol.37, no.1, pp.426-433, 2010.